(2)

MTL TR 92-65

AD

EVALUATION OF THE MODIFIED FORWARD HMMWV LIFT PROVISION IN DUAL SIDE-BY-SIDE AIRLIFT CONFIGURATIONS

ROBERT B. DOOLEY, PAUL V. CAVALLARO,
KRISTEN D. WEIGHT, and CHRISTOPHER CAVALLARO
MECHANICS AND STRUCTURES BRANCH

September 1992

Approved for public release; distribution unlimited.

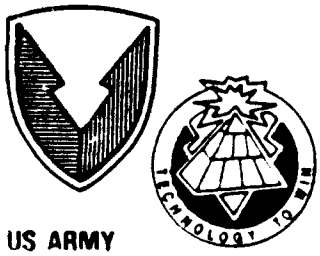

US ARMY
LABORATORY COMMAND
MATERIALS TECHNOLOGY LABORATORY

Sponsored by
U.S. Natick Research, Developement, and Engineering Center
Natick, MA

U.S. ARMY MATERIALS TECHNOLOGY LABORATORY
Watertown, Massachusetts 02172-0001

The findings in this report are not to be construed as an official Department of the Army position, unless so designated by other authorized documents.

Mention of any trade names or manufacturers in this report shall not be construed as advertising nor as an official indorsement or approval of such products or companies by the United States Government.

DISPOSITION INSTRUCTIONS

Destroy this report when it is no longer needed.
Do not return it to the originator

UNCLASSIFIED

SECURITY CLASSIFICATION OF THIS PAGE (When Data Entered)

REPORT DOCUMENTATION PAGE		READ INSTRUCTIONS BEFORE COMPLETING FORM
1. REPORT NUMBER NTL TR 92-65	2. GOVT ACCESSION NO.	3. RECIPIENT'S CATALOG NUMBER
4. TITLE (and Subtitle) EVALUATION OF THE MODIFIED FORWARD HMMWV LIFT PROVISION IN DUAL SIDE-BY-SIDE AIRLIFT CONFIGURATIONS		5. TYPE OF REPORT & PERIOD COVERED Final Report 6. PERFORMING ORG. REPORT NUMBER
7. AUTHOR(s) Robert B. Dooley, Paul V. Cavallaro, Kristen D. Weight, and Christopher Cavallaro		8. CONTRACT OR GRANT NUMBER(s)
9. PERFORMING ORGANIZATION NAME AND ADDRESS U.S. Army Materials Technology Laboratory Watertown, Massachusetts 02172-0001 ATTN: SLCMT-MRS		10. PROGRAM ELEMENT, PROJECT, TASK AREA & WORK UNIT NUMBERS D/A Project 1L162105AH84
11. CONTROLLING OFFICE NAME AND ADDRESS U.S. Army Natick Research, Development, and Engineering Center Natick, Massachusetts 01760-5010		12. REPORT DATE September 1992 13. NUMBER OF PAGES 35
14. MONITORING AGENCY NAME & ADDRESS(if different from Controlling Office)		15. SECURITY CLASS. (of this report) Unclassified 15a. DECLASSIFICATION/DOWNGRADING SCHEDULE

16. DISTRIBUTION STATEMENT (of this Report)

Approved for public release; distribution unlimited.

17. DISTRIBUTION STATEMENT (of the abstract entered in Block 20, if different from Report)

18. SUPPLEMENTARY NOTES

19. KEY WORDS (Continue on reverse side if necessary and identify by block number)

High mobility multipurpose wheeled vehicles (HMMWV)
External airlift transport (EAT)
Airlift configuration
Field tests
Finite element analysis

20. ABSTRACT (Continue on reverse side if necessary and identify by block number)

(SEE REVERSE SIDE)

DD FORM 1 JAN 73 1473 EDITION OF 1 NOV 65 IS OBSOLETE

UNCLASSIFIED

SECURITY CLASSIFICATION OF THIS PAGE (When Data Entered)

Block No. 20

ABSTRACT

Field modifications to U.S. Army External Airlift Transport (EAT) operating procedures became critically necessary during Operation Desert Storm. To meet mission essential objectives, the U.S. Army 101st Airborne Division developed a new dual side-by-side (DSS) airlift sling configuration for airlifting two high mobility multipurpose wheeled vehicles (HMMWV) simultaneously with a CH-47D helicopter. The U.S. Army Materials Technology Laboratory performed experimental and finite element analysis (FEA) activities to evaluate the performance of the forward outboard HMMWV lift provisions subjected to DSS sling configurations. These activities were performed at the request of the Natick Research, Development, and Engineering Center in an attempt to certify two DSS airlift configurations under consideration for further use. Results of both the experimental and analytical analyses were obtained, discussed, and subsequently correlated. Conformity of the provision to Military Standard 209-G, "Slinging and Tiedown Provisions for Lifting and Tying Down Military Equipment" was evaluated for both configurations.

CONTENTS

INTRODUCTION

An Army External Airlift Transport (EAT) procedure for ground vehicles consists of a CH-47D helicopter transporting two HMMWVs in the tandem configuration depicted in Figure 1. The CH-47D employs a pair of fore and aft lift points. Each lift point supports an individual vehicle using four sling/chain assemblies. Opposite ends of the sling/chain assemblies are attached to the two front airlift provisions and the two rear bumper shackles of each HMMWV.

Photograph, courtesy of ARMED FORCES JOURNAL INTERNATIONAL, April, 1992.

Figure 1. CH-47D lifting 2 HMMWVs in tandem configuration.

The tandem configuration was found to interfere with the operation of the CH-47D altimeter. Signals emitted from the altimeter system reflected off the forward positioned HMMWV rather than the ground resulting in erroneous altitude readings. Interference of this type poses a serious threat to the safety of both the pilot and crew, particularly during low altitude night operations.

In an effort to alleviate the altimeter interference problem, the 101st Airborne Division designed and employed a new, uncertified Dual Side-by-Side (DSS) lift configuration as illustrated by Figure 2. Sling rigging procedures for this configuration applied a significantly increased out-of-plane bending load to the forward outboard (FO) HMMWV lift hooks as compared to both the single and tandem airlift configurations. Airlift provisions in all cases are required to conform to MILITARY STANDARD 209G (MIL-STD-209G) "Slinging and Tiedown Provisions for Lifting and Tying Down Military Equipment"[1]. Specifically, no lift provision may plastically deform (yield) as a result of a sling force application up to and including 3.2 times the effective working static load of the individual sling (3.2g).

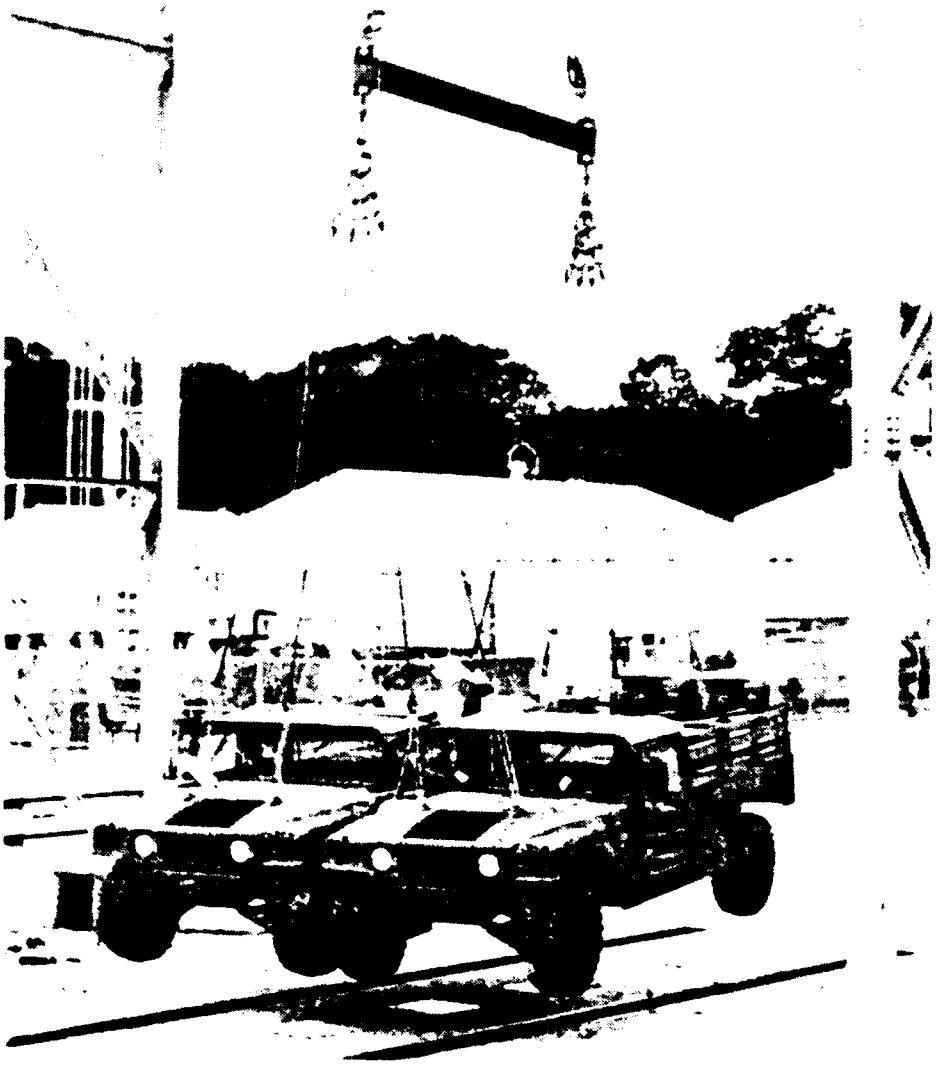

Figure 2. DSS airlift configuration.

Two DSS configurations, referred to herein as the 101st and NRDEC configurations, were evaluated to determine if conformity of the FO lift provision to MIL-STD-209G was maintained. Static suspension tests were performed to characterize sling force vectors required for Finite Element Analysis (FEA) of the provision. Strain gages were mounted at various locations to report the strain response of the provision to static 1.0g loads. Experimental strain gage results were correlated with the FEA model results and were used to qualify the models for provision evaluation.

DESCRIPTION OF HHV AIRLIFT PROVISION

Since first introduced to military service, the HMMWV has been upgraded and modified as specific applications require. In recent years, heavier payloads requiring increased lift provision strength have resulted in design modifications to critical airlift components.

The Heavy HMMWV Variant (HHV) is an up-weighted HMMWV for light tactical, utility, combat, and scouting operations. Among the many design improvements to this HMMWV version are the forward airlift provisions. As a result of increased Gross Vehicle Weight (GVW), original airlift provisions were rendered insufficient for certain air mobile unit operations. HHVs with their modified forward lift hooks are appropriate for heavy external air transport operations and were used during all testing and analysis activities in this investigation.

Lift Provision Construction

As illustrated in Figure 3, the HHV modified forward airlift provision is constructed of a 0.75" diameter inverted "U" shaped rod welded at both ends to opposite corners of a 3.00" X 4.00" X 20.375" main bracket box beam. A 0.25" thick reinforcement plate is welded to the straight sections of the rod to provide additional stiffness, thereby diminishing the effect of in-plane bending stresses within these sections. Adjacent to the main box beam are two end-beveled "C" channels. The channel beams are welded adjacent to each other and finally to the box beam. The three beam sections together are referred to as the bracket section of the provision and are mechanically fastened to the HHV frame by ten (10) 5/8" diameter bolts. All components of the assembly, (bracket and hook) are made of 1020 cold drawn steel.

In comparison to the modified HHV forward lift provision, the original consists of a 0.625" diameter rod and does not include the 0.25" thick reinforcement plate.

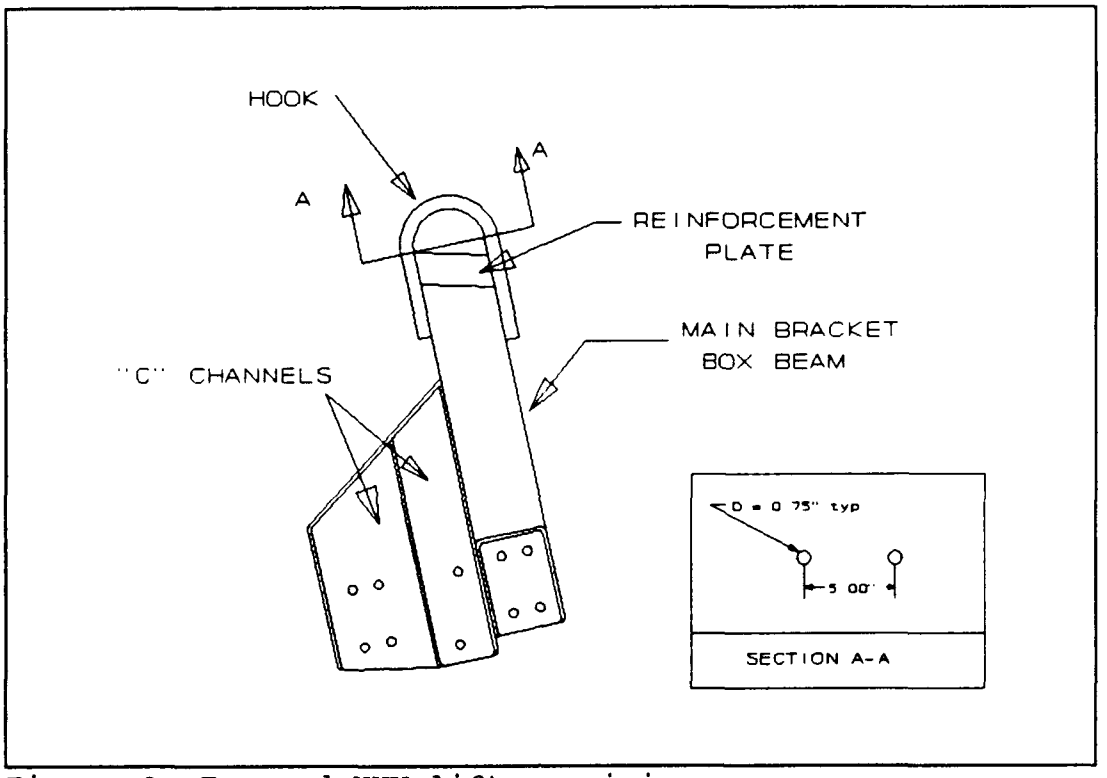

Figure 3. Forward HHV lift provision.

Lift Hook Loading Design Criteria

An assessment of the in-plane and transverse normal bending stiffnesses, EI_{ii} and EI_{tt} respectively, for the HHV provisions was performed. Referring to Figure 3, β is defined as the ratio of the in-plane to the transverse normal moments of inertia along section A-A for the in-plane and out-of-plane directions. The following value of β was computed for the forward HHV provision:

$$\beta_{HHV} = (I_{ii} / I_{tt})_{HHV} = 172.54 \qquad (1)$$

Since β is much greater than 1.0, the flexural stiffness in the in-plane direction is much greater than the stiffness in the out-of-plane direction (β for the standard HMMWV provision is 248.34). These results indicate that the hook was designed primarily for in-plane loads.

As a consequence of the position of the FO provision relative to the vertical configuration centerline, worst case (highest combination of bending and axial loads) provision sling loading was anticipated for the outboard provision. Sling loading vectors collinear with the longitudinal axis of the main bracket box beam minimize bending stresses within the "U" shaped rod and are therefore

at desirable orientations. Slings loading the FO provisions in DSS configurations are oriented at angles which tend to bend the hooks inwards towards the vehicle center. In addition, FO sling forces require higher magnitudes to achieve a vertical force component equal to the vertical component of the forward inboard sling.

These findings are consistent with hook loading procedures as outlined in MIL-STD-209G. For the 10,000 lb GVW class HHV test vehicles used, loading of the hook should be primarily in the in-plane direction and as close to the box beam centerline as possible.

SIMULATED AIRLIFT TESTS

Simulated DSS airlift tests were performed to characterize the FO sling force vector (directions and magnitude) and to record the strain response of the provision to static 1.0g loads.

Simulated Airlift Test Procedure

DSS simulation tests were performed by suspending two 10,000 lb HHVs from an "I" beam fixture supported by an overhead crane (Figure 2). A 160 inch long "I" beam was used to simulate the distance between the fore and aft lift points of the CH-47D. Shackles were fixed to both ends of the beam to support the forward and rear vehicle slings.

Prior to testing, both HHVs were positioned parallel to each other, facing the same direction, and were separated by approximately six (6) inches. Two 3 inch thick corrugated cardboard honeycomb panels were placed between the HHVs to distribute vehicle contact forces and to protect the HHV side panels. Load cells were mounted in series between the beam shackles and the lift slings to measure forward outboard and forward inboard sling forces throughout the tests.

Sling force and strain data acquisition systems were triggered to record prior to lifting. These systems remained active through the suspension period while angle measurements were recorded. Termination of data recording occurred only after the vehicles returned to the ground and the lift slings supported no weight.

CHARACTERIZATION OF DSS AIRLIFT CONFIGURATIONS

Differences between the two DSS configurations are primarily the result of the user preferred vehicle nose down angle, as illustrated in Figure 4. Vehicle symmetry, with respect to the longitudinal axis of the helicopter, is

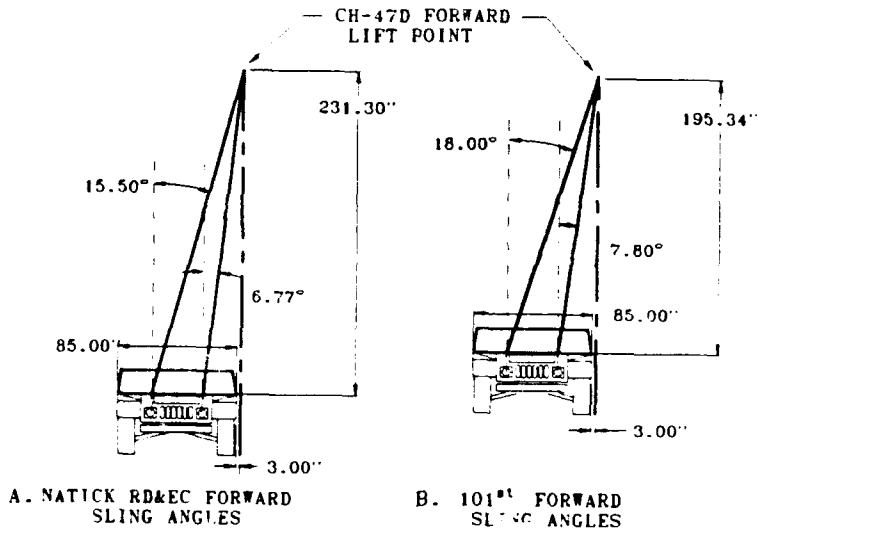

A. NATICK RD&EC FORWARD SLING ANGLES

B. 101st FORWARD SLING ANGLES

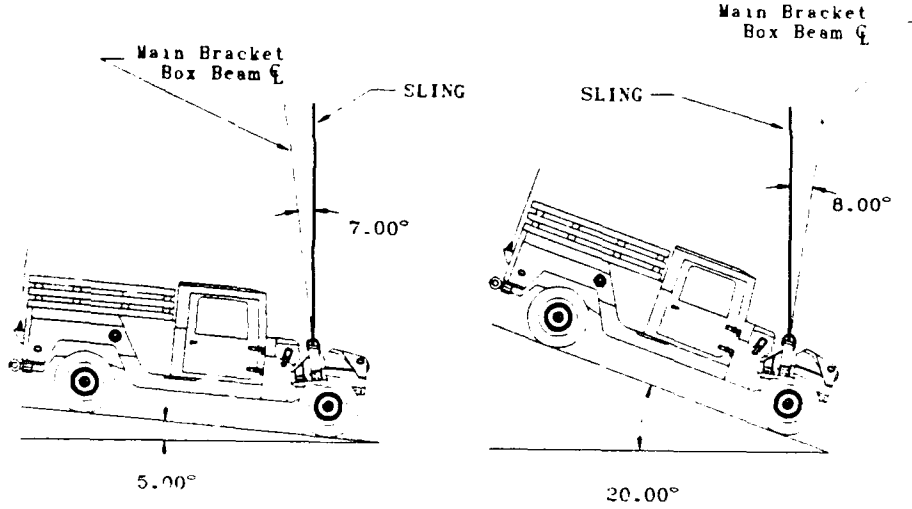

C. NRDEC Side Angles

D. 101st Side Angles

Figure 4. Front and side view of sling angles relative to vehicles in both the 101st and NRDEC configurations.

required for weight distribution (flight stability) and is common to both configurations. Nose down angles and vehicle symmetry are both achieved by adjusting each sling/chain to predetermined lengths prior to attachment to the helicopter. For each configuration, the required sling/chain assembly lengths vary according to vehicle lift point location. Length adjustments are made secure by passing the sling chain through the hook and sliding the appropriate chain link into the yoke of a link keeper (slotted shackle).

Results of Configuration Characterization

Results of angle measurements taken during testing are illustrated in Figure 5. Forward outboard sling angles were measured with an inclinometer placed collinearly along the sling, and were recorded relative to both the horizontal and vertical. Forward inboard angles were calculated based on FO sling angles and vehicle geometry. Together, the longitudinal and transverse angles uniquely characterize the orientation of the forward outboard sling relative to a coordinate axes system originating at the sling/hook contact point.

Sling force data, as reported by the load cells, were used in conjunction with angle measurements to resolve the FO sling force into equivalent sets of three mutually orthogonal components as shown in Figure 5 (see Appendix I for sling force resolution calculations). Tables 1 and 2 below summarize the component results.

Table 1. DSS RESOLVED FORCES
(Forward Outboard Sling)

	101ST	NRDEC
FO Sling force (lb.)	2913	2435
Fx (lb.)	-617	97
Fy (lb.)	2746	2330
Fz (lb.)	751	700
Angle front (deg.)	72.0	74.5
Angle side* (deg.)	8.0	-7.0
Nose down angle (deg.)	20.0	5.0

*(Side angle includes -12° provision mounting angle)

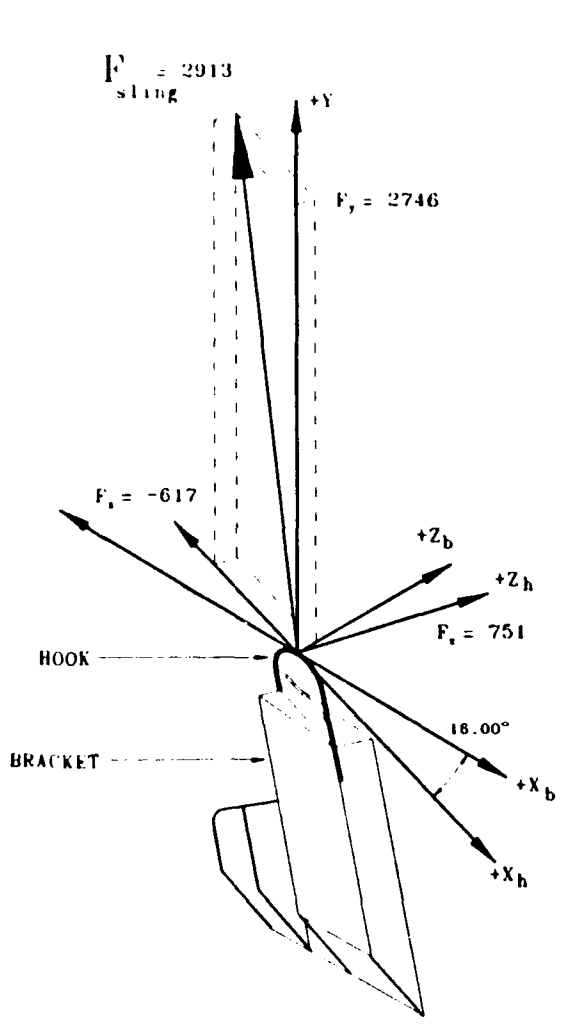

101st Force Resolution

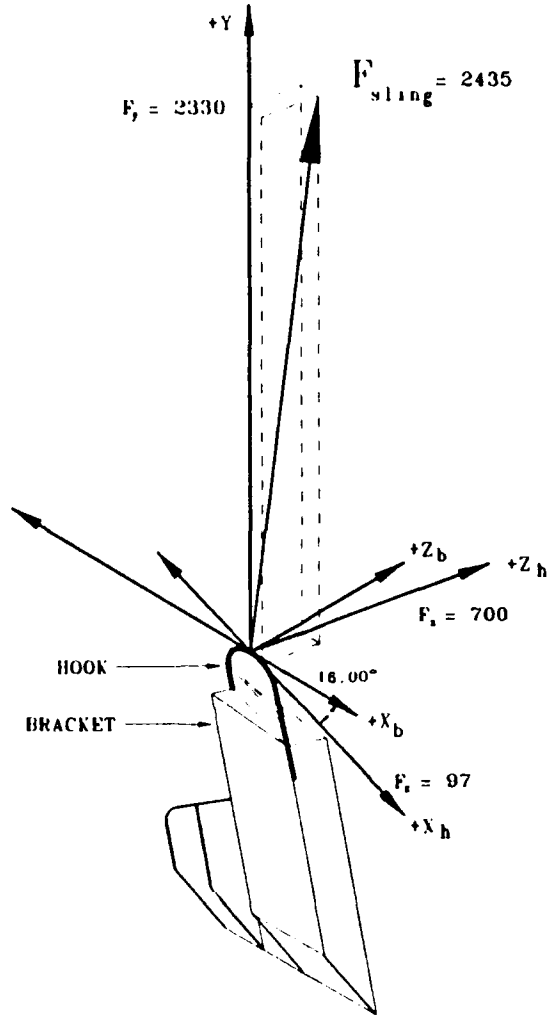

NRDEC Force Resolution

"h" = hook coordinate system
"b" = bracket coordinate system

Figure 5. Sling angles relative to the hock contact point of the FO provision.

Table 2. DSS RESOLVED FORCES
(Forward Inboard Sling)

	101ST	NRDEC
FI Sling force (lb.)	1772	2363
Fx (lb.)	301	199
Fy (lb.)	1739	2329
Fz (ib.)	162	345
Angle front (deg.)	82.2	83.2
Angle side* (deg.)	8.0	-7.0
Nose down angle (deg.)	20.0	5.0

*(Side angle includes -12° provision mounting angle)

Expressing the FO sling force components in parametric form yields the following equations;

For 1.0g forces

$$101^{st} \text{ Config.} \quad F = -617x_i + 2746y_j + 751z_k$$
$$\text{NRDEC Config.} \quad F = 97x_i + 2330y_j + 700z_k$$

At 3.2g, the force vectors become

$$101^{st} \text{ Config.} \quad F = -1974x_i + 8787y_j + 2403z_k$$
$$\text{NRDEC Config.} \quad F = 310x_i + 7456y_j + 2240z_k$$

STRAIN DATA ACQUISITION

A total of fifteen Micro-Measurements (TM) type EA-13-125EP-350 uniaxial strain gages were mounted to the hook and bracket sections of the forward outboard lift provision. Figure 6 illustrates the approximate locations of each gage relative to the provision. Gages number 1 through 5 were mounted on the inner web surfaces of the two "C" channel beams of the provision bracket. The remaining ten gages (gages No.s 6-15) were reserved for the hook and were positioned to coincide with predetermined FEA model integration point locations.

A MEGADAC Series 2000 (TM) multi-channel data acquisition system was used to record strain gage signals at a scan rate of 120 samples per second, per channel. Each gage occupied an individual system channel with additional channels reporting elapsed and cumulative time.

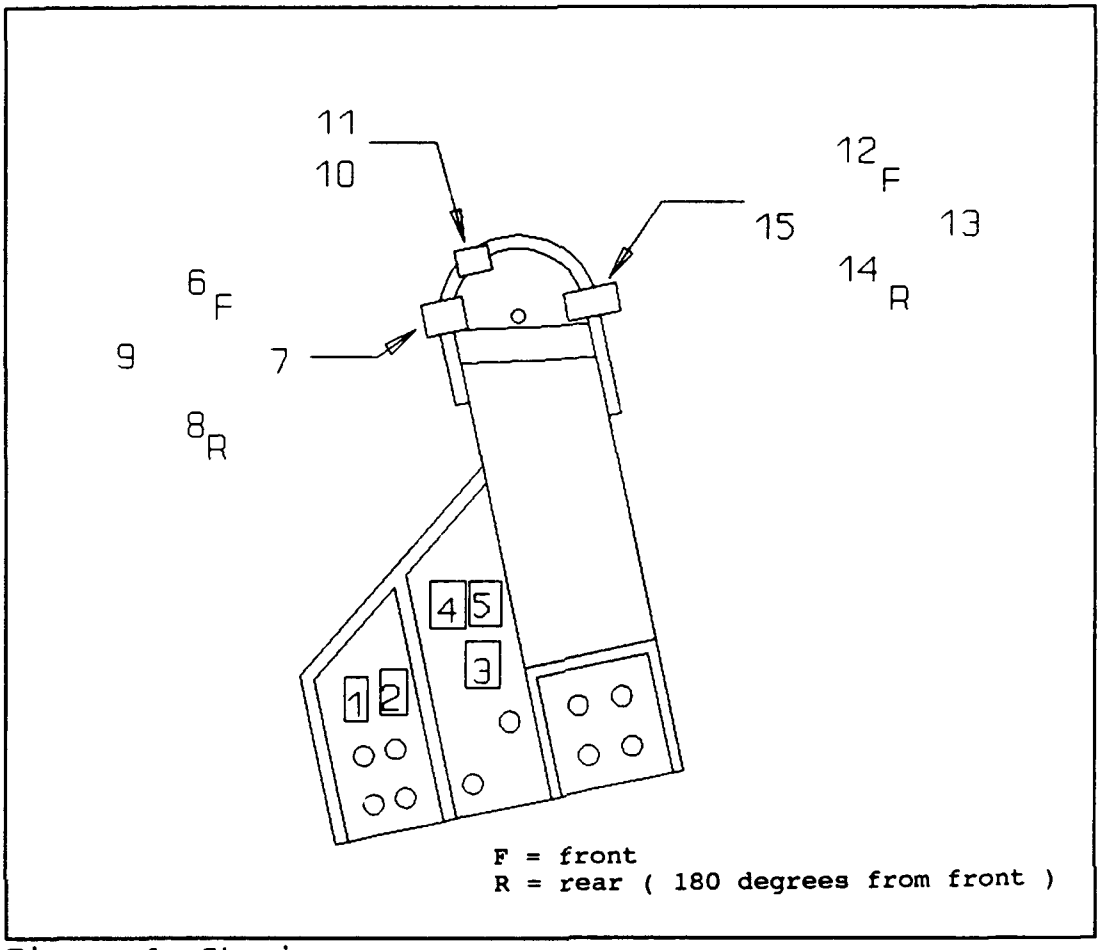

Figure 6. Strain gage map.

System recording was triggered by means of the host computer using OPUS (TM) software. A "zero load" test file was recorded prior to lifting the vehicles to obtain strain transducer offset values after balancing and calibrating all data acquisition system channels. These values were used to compensate for the offsets of each strain gage on a channel by channel basis as necessary.

The tests performed are listed in Table 3 according to the sling configurations tested and the order in which they occurred.

Table 3. STRAIN DATA TEST FILES

TEST #/FILE EXT.	DESCRIPTION
1 / R01	Zero Values
2 / R03	101st
3 / R04	101st
4 / R05	NRDEC

Strain Data Processing and Results

Strain gage results obtained from suspension tests were individually plotted (60 plots = 4 tests with 15 channels per test) with microstrain as the ordinate (Y-axis), and elapsed time in minutes as the abscissa (X-axis). These plots represent the axial strain reported by each gage as a function of time and show the strain response of the hook and provision through the lifting, static suspension, and unloading portions of each test.

To determine the average digital values of the plotted strain, five samples of data were extracted from each gage file. The first and last samples consisted of approximately 100 data points each and correspond to pre and post vehicle lifting. These samples were used to determine residual strains ($\delta\epsilon$) in the provision by comparing initial sample average to final sample average strain values.

Sample numbers 2, 3, and 4 consisted of approximately 500 points each and were taken at the beginning, middle and end of vehicle suspension respectively. Statistical analysis of these three samples were used to obtain the average maximum (tension) or minimum (compression) values of strain for each gage in both test configurations. The "+/-" column computed for both configuration tests reports the average of standard deviations from samples 2, 3, and 4 of each strain gage. Results of the statistical analysis are summarized in Table 4.

Table 4. STRAIN GAGE RESULTS.

Descrip.	Zero Values		101st Config.			NRDEC Config.		
	($\mu\epsilon$)		($\mu\epsilon$)			($\mu\epsilon$)		
Gage #	Ave.	+/-	Ave.	+/-	$\delta\epsilon$	Ave.	+/-	$\delta\epsilon$
1.	-20	22	-137	3	-16	-105	21	4
2.	-18	22	-109	3	-16	-80	21	4
3.	-18	22	22	3	-20	10	23	-4
4.	-19	22	-95	3	-7	-89	21	4
5.	-18	22	-102	3	-7	-95	21	5
6.	-18	22	922	5	-5	794	44	1
7.	-18	22	522	5	-9	388	33	-23
8.	-35	22	-772	11	1	-661	17	38
9.	-23	22	151	3	-4	-91	21	3
10.	-21	22	260	3	-12	319	31	-22
11.	-19	22	-64	3	3	-123	20	9
12.	-21	22	883	3	-6	752	46	-44
13.	-19	22	113	3	-5	18	28	1
14.	-14	22	-671	3	0	-593	17	38
15.	-17	22	312	3	0	281	30	-14

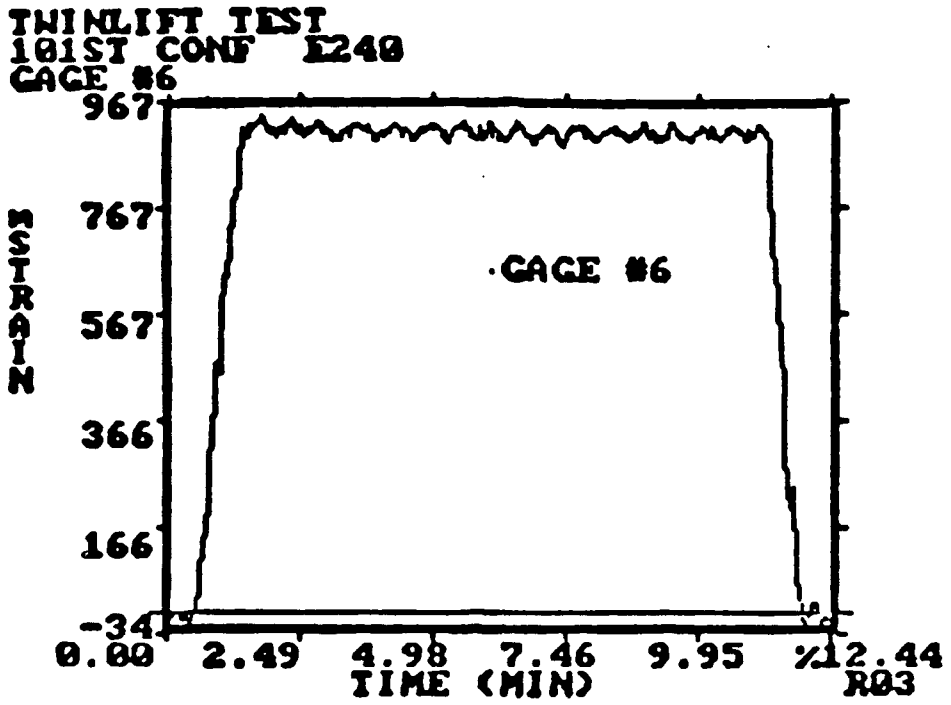

#	Statistic	Value
1	Count (N)	499.000000
2	Sum	457818.299600
3	Mean	917.471542
4	SEM (s.e. of mean)	0.566418
5	Median	917.058900
6	Variance	160.094059
7	StDev (sd)	12.652828
8	Maximum	949.411900
9	Minimum	891.176600
10	Range	58.235300
11	Skewness	0.009864
12	Kurtosis	-1.284136

Figure 7. Strain versus elapsed time plot for strain gage #6, test #2 (statistics of sample # 3 included).

A sample plot of gage number 6, test file number 2 is shown in Figure 7 with the results of a statistical analysis of one of five samples (in this case, sample #3) taken per plot. Figure 8 shows the five locations at which the samples were taken. Statistical average values obtained from samples number 2, 3, and 4 were again averaged to yield a single representative value of strain for each gage during the static suspension portion of each test.

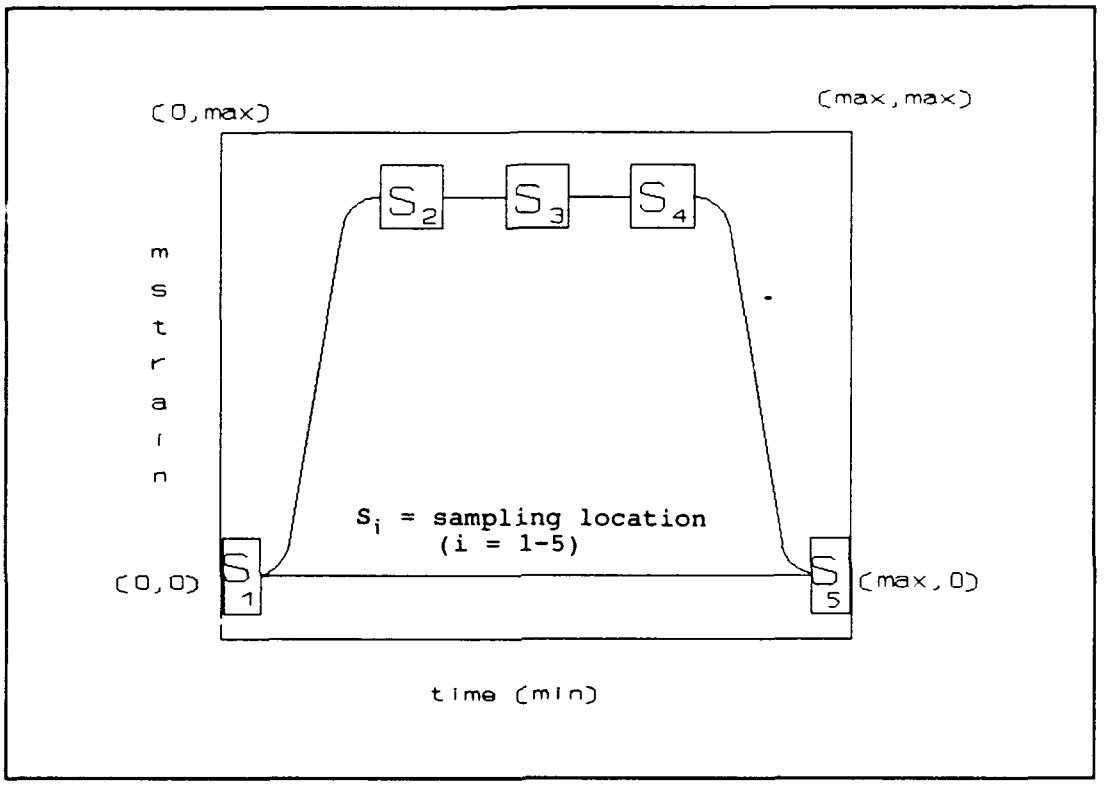

Figure 8. Typical sampling locations of strain plot.

Strain gage data from test file number 3 (corresponding to the 2nd 101st lift test) was not processed in the manner described above. This file was recorded after the data storage media tape for the first two tests was removed from the test system and replaced by a second new tape. A brief lift test (test number 3, data storage tape number 2) was performed during which time the suspended vehicles swung back and forth in a pendulum type motion. The vehicles were returned to the ground before the swinging motion subsided and was therefore not a true suspension test. The purpose of performing this test was primarily to ensure that the new tape was properly formatted and that the system was functioning properly.

FINITE ELEMENT ANALYSES

In order to determine the response of the outboard HHV provision to the loading cases shown in Figure 5, finite

element analyses of both the hook and bracket were performed. Preliminary linear elastic analyses predicted the existence of plasticity within the U-shaped hook component of the outboard provision. Stresses obtained from these models exceeded the material yield strength (σ_y = 87,500 psi) at 3.2 times the magnitude of the static loading vector for both the 101st and NRDEC load cases. These models are shown in Figure 9.

Modeling efforts were then focused on the development of a 3 dimensional, elastic-plastic finite element representation of the complete provision to detect possible plastic deformation throughout the hook and bracket sections. The elastic-plastic model was generated by using the PATRAN[2] (TM) preprocessor and analyzed with the ABAQUS[3] (TM) commercial code. This model revealed that stresses within the bracket section of the provision were relatively low in comparison to the hook component.

Linear Elastic Hook Finite Element Models

Hook models of the 101st and NRDEC FO provision shown in Figure 9 were restricted to the portion of the hook located above the reinforcement plate (refer to Figure 3). Sections below the reinforcement plate were not modeled since (1) stresses resulting from the applied loads were distributed locally between the hook and the vertical welds of the reinforcement plate, (2) significant increases in axial, bending, and shear stiffnesses existed at the weld regions and (3) stresses within the hook section located below the reinforcement plate were minimal.

Hook models were constructed of ABAQUS^{tm} Type B31 beam elements. These two noded, 3 dimensional isoparametric elements assume a linearized displacement field in $\{u,v,w,\theta\}$ with integration points (I.P.,finite points, the locations of which report results) located as shown in Figure 10.

Boundary conditions fixing the translational and rotational degrees of freedom (DOFs) were imposed on nodes located at the top of the welds connecting the hook to the reinforcement plate as shown in Figure 9. Justification for these boundary assumptions were based on the significant increases in axial, bending, and shear stiffnesses at the welds. Loading vectors representing the outboard slings were described for each DSS case by the parametric equations indicated.

The vectors were applied to the models as concentrated forces to simulate the worst case condition as in previous investigations[4]. Contact at the chain/hook interface was modeled as only one edge of one link, in contrast to the combination of one edge and one face of two individual links as shown in Figure 11.

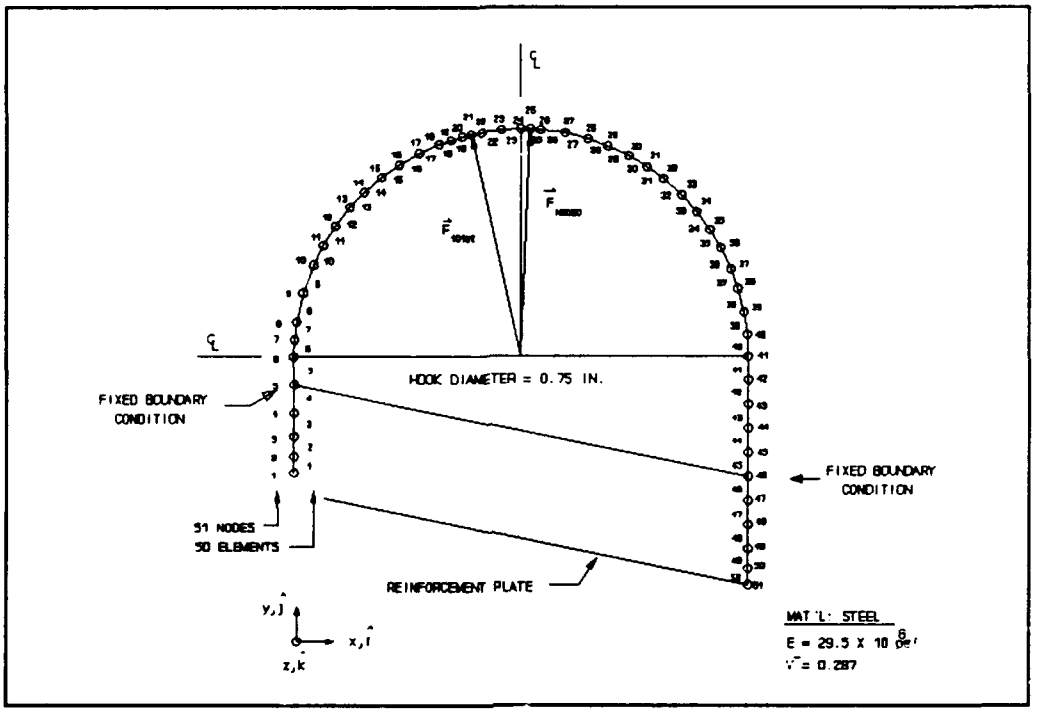

Figure 9. Linear elastic FEA mesh of provision hook.

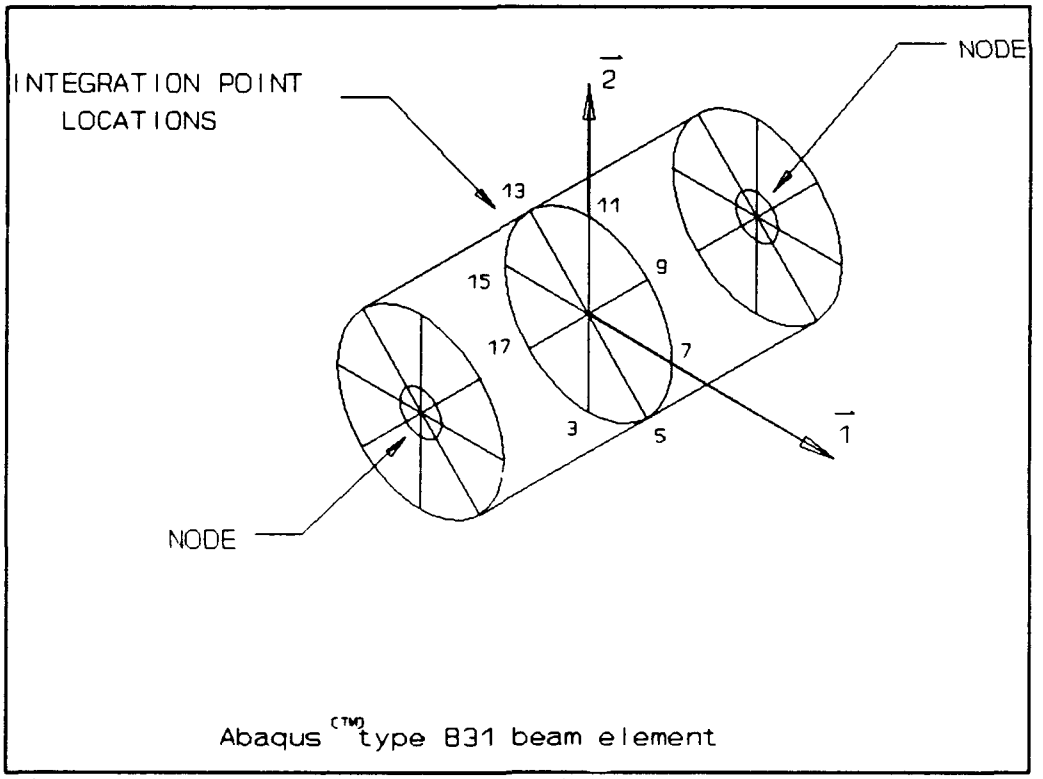

Figure 10. Integration point locations of beam element.

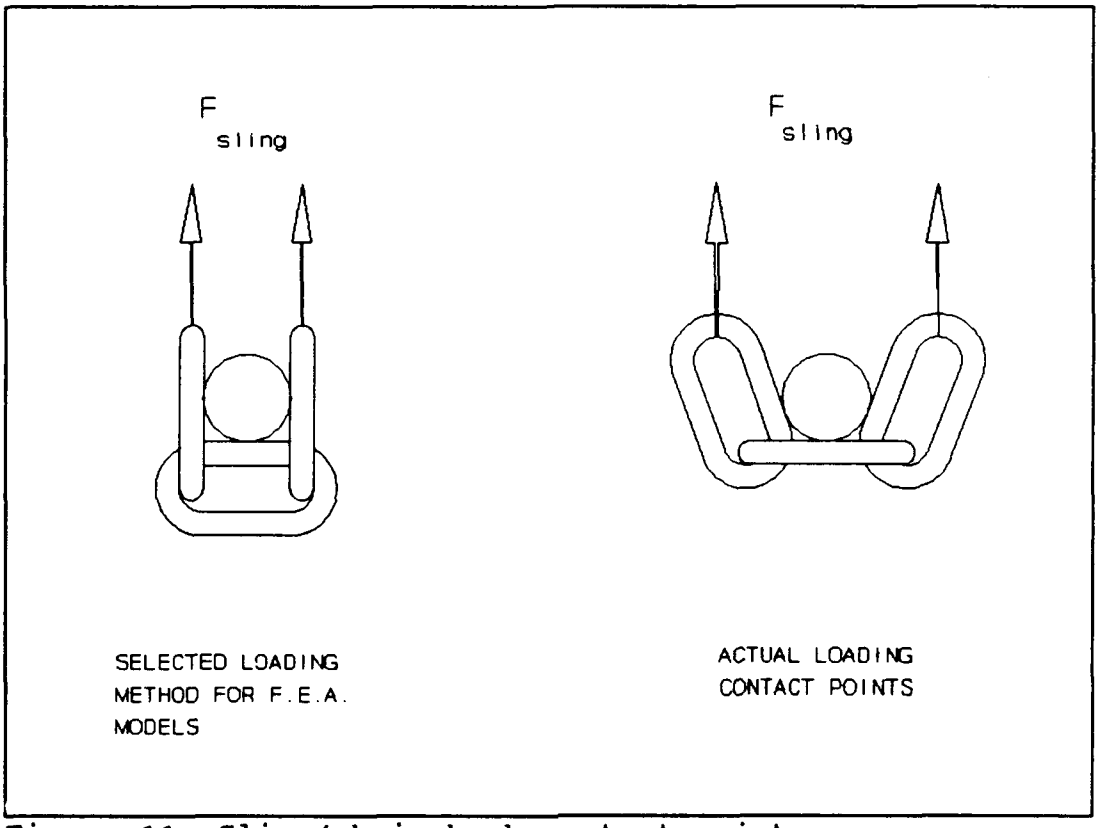

Figure 11. Sling/chain hook contact points.

Results of Linear-Elastic Hook Finite Element Models

Results for the 101st and NRDEC cases were obtained using a sling force load of 3.2 times the measured 1.0g sling force (indicated force vectors in Figure 5) and are displayed in Figures 12 and 13 for the 101st and NRDEC configurations respectively. Axial strains, ϵ , are plotted over the curved section of the hook as a function of the angle ϕ, where ϕ is defined as the angle between the line connecting the element midpoint to the center of the hook's curved section. Each strain plot consists of four curves, one curve for each of the four integration points (# 3,7,11,15) on the midpoint cross section of each element.

Correlation of Linear-Elastic FEA Model Results to Experimental Results

Strain gage results obtained from the simulated DSS airlift tests were multiplied by a factor of 3.2 and positioned on the corresponding locations of the curves in Figures 12 and 13. A yield strain value of 2.966E-03 in/in obtained from previous material characterization tests was

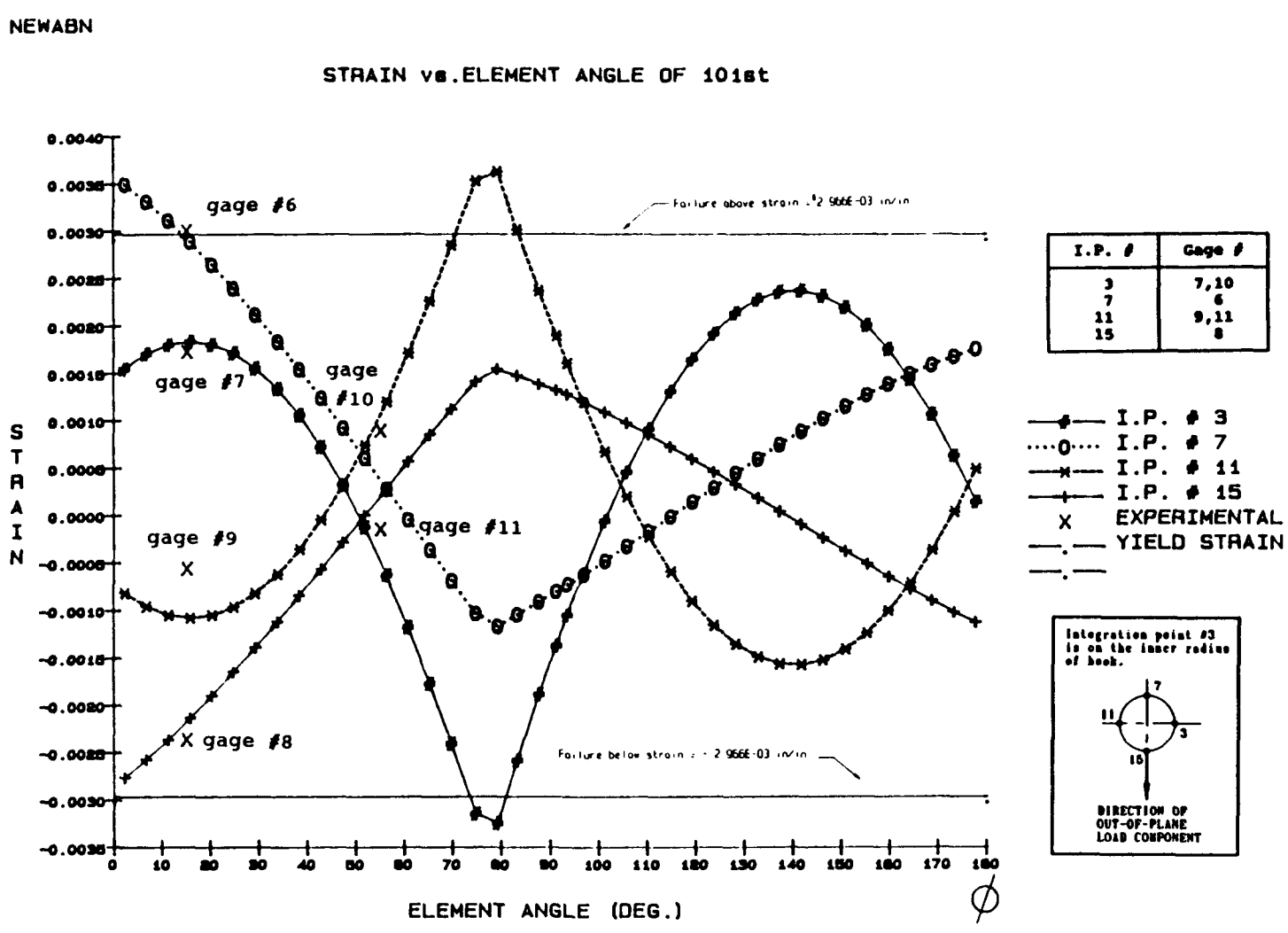

Figure 12. Linear elastic FEA results for 101st configuration model loaded with 3.2g sling force. Strain gage results multiplied by 3.2 and positioned accordingly.

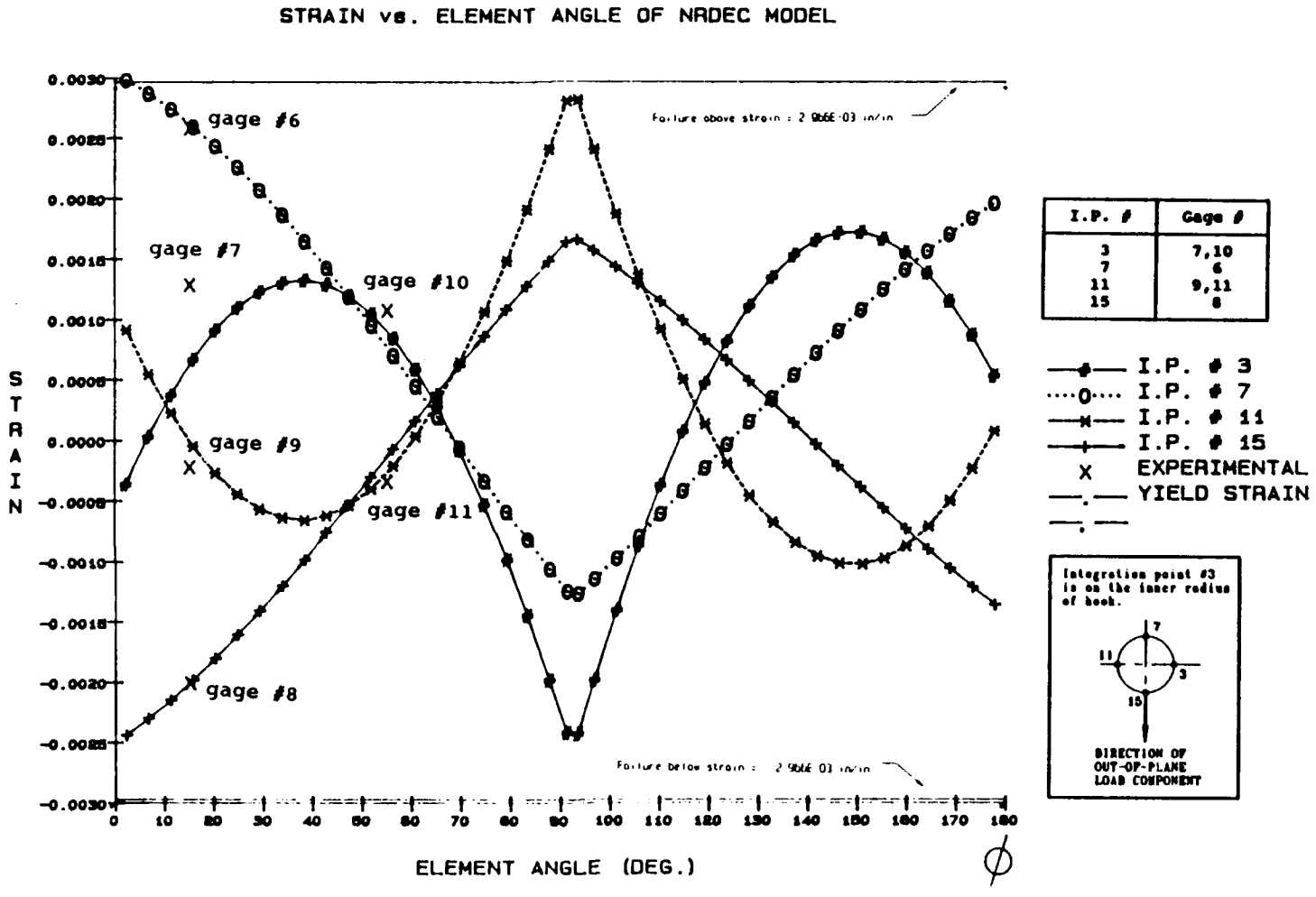

Figure 13. Linear elastic FEA results for NRDEC configuration model loaded with 3.2g sling force. Strain gage results multiplied by 3.2 and positioned accordingly.

used to indicate model yielding[5]. This constant value was plotted for both tension and compression in both configuration cases from ϕ = 0.0° to ϕ = 180°. Model strain results of a magnitude greater than ϵ = +2.966E-03 or less than ϵ = -2.966E-03 indicate material yielding at 3.2g sling forces.

Linear elastic FEA strain result plots indicate that both configurations yield below the required 3.2g sling force limit. Strain gage data plotted on the curves in Figures 12 and 13 demonstrate the degree of correlation between experimental and F.E.A. results. These plots indicate that the magnitude of strain within the hook exceeds acceptable limits.

Elastic Plastic Full Provision Finite Element Model

An elastic plastic finite element analysis of the full provision (bracket and hook) was performed on the model shown in Figure 14.

The model is constructed of ABAQUS (TM) Type B31 two noded beam elements throughout the hook portion of the model with ABAQUS (TM) S4R Type four noded shell elements throughout the bracket section of the provision (with isotropic hardening, plastic strain data obtained from previous tests).

Attachment of the hook to the bracket was accomplished by means of multiple point constraints between neighboring nodes of the hook and bracket interface. This method provides rigid beam attachments between the nodes of the hook and nodes of the bracket resulting in equivalent displacements and rotations to approximate the weld interface. Rigid body displacement of the model was prevented by fixing translational and rotational degrees of freedom at the 10 node locations corresponding to the vehicle frame bolt holes.

Sling force loading of the model was performed with 1.0g loads determined during testing and resolved in a manner similar to the linear elastic model case. Application of the force to the hook occurred at a single representative node for each of the two cases (chain hook interface assumptions similar to the linear elastic model).

Elastic-Plastic Model Results

Results of the elastic-plastic FEA model were evaluated, and correlated with experimental results, in a manner identical to the linear elastic model method.

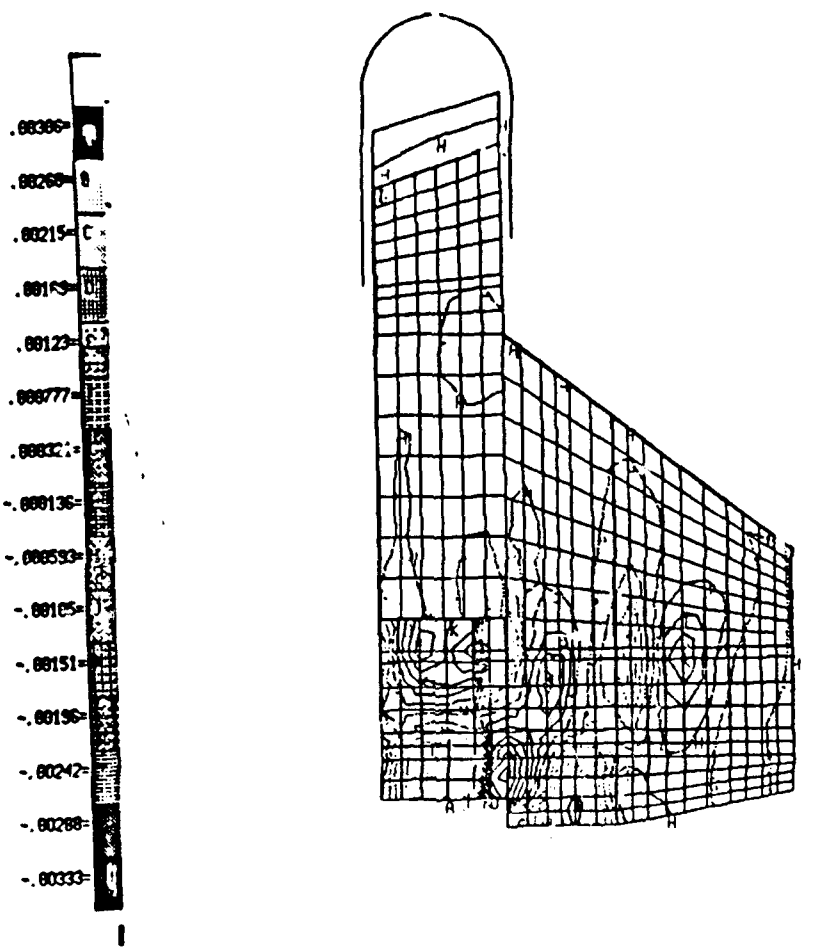

Figure 14. Elastic-plastic tull provision FEA mesh.

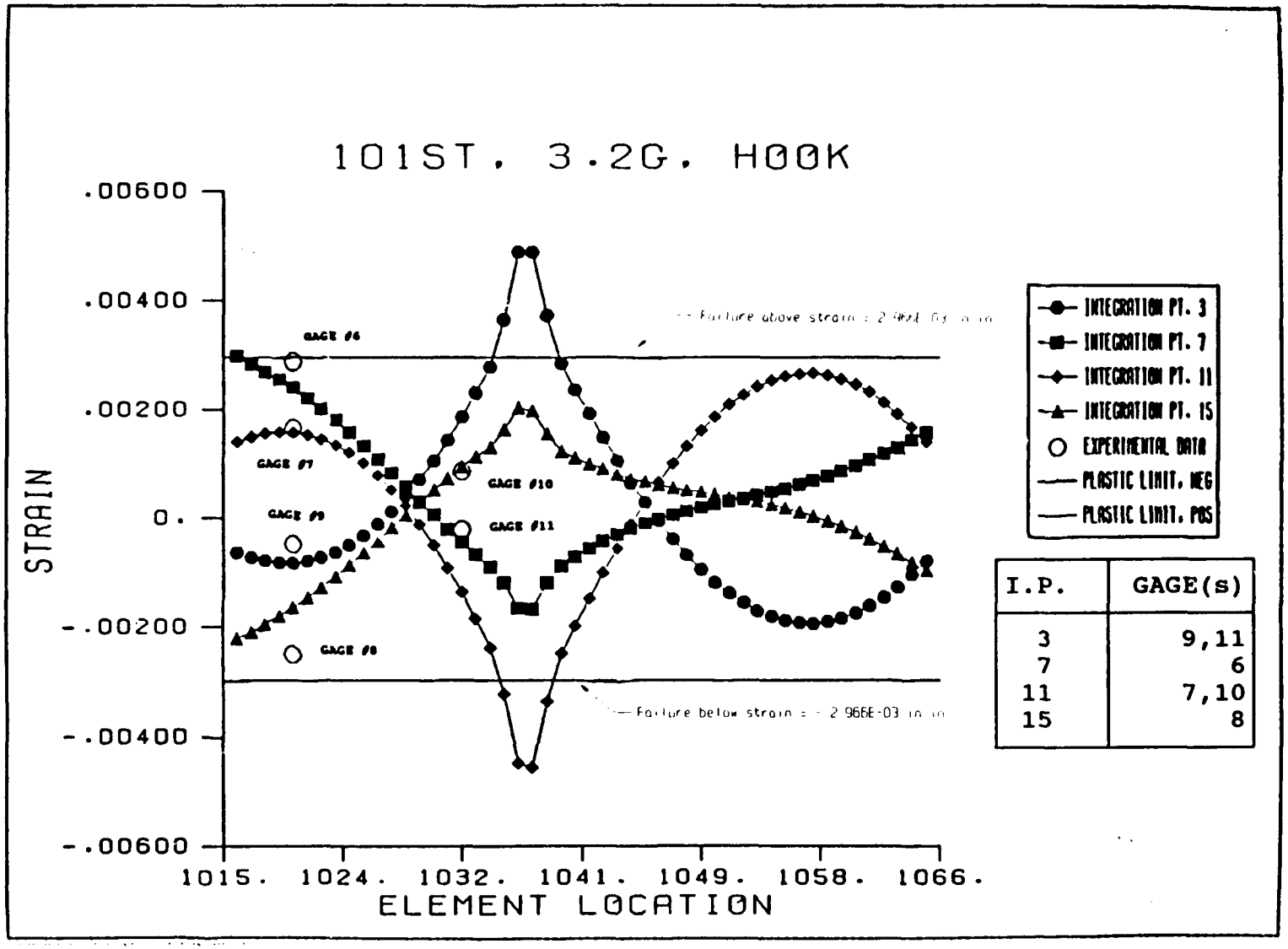

Figure 15. Results of elastic-plastic FEA of hook portion of FO provision in 101st configuration. Strain versus element number at 3.2g with strain gage results superimposed at 3.2g.

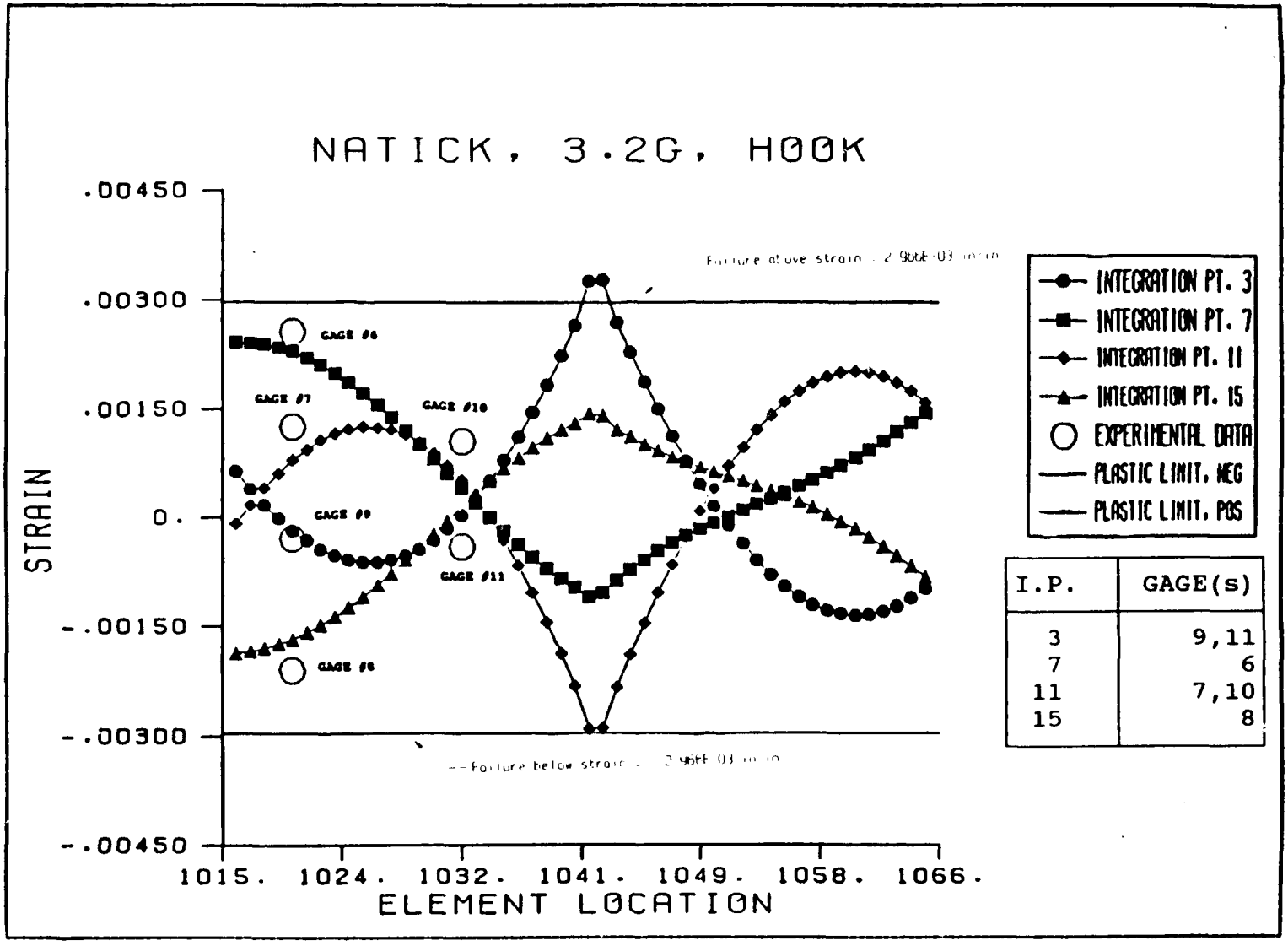

Figure 16. Results of elastic-plastic FEA of hook portion of FO provision in NRDEC configuration. Strain versus element number at 3.2g with strain gage results superimposed at 3.2g.

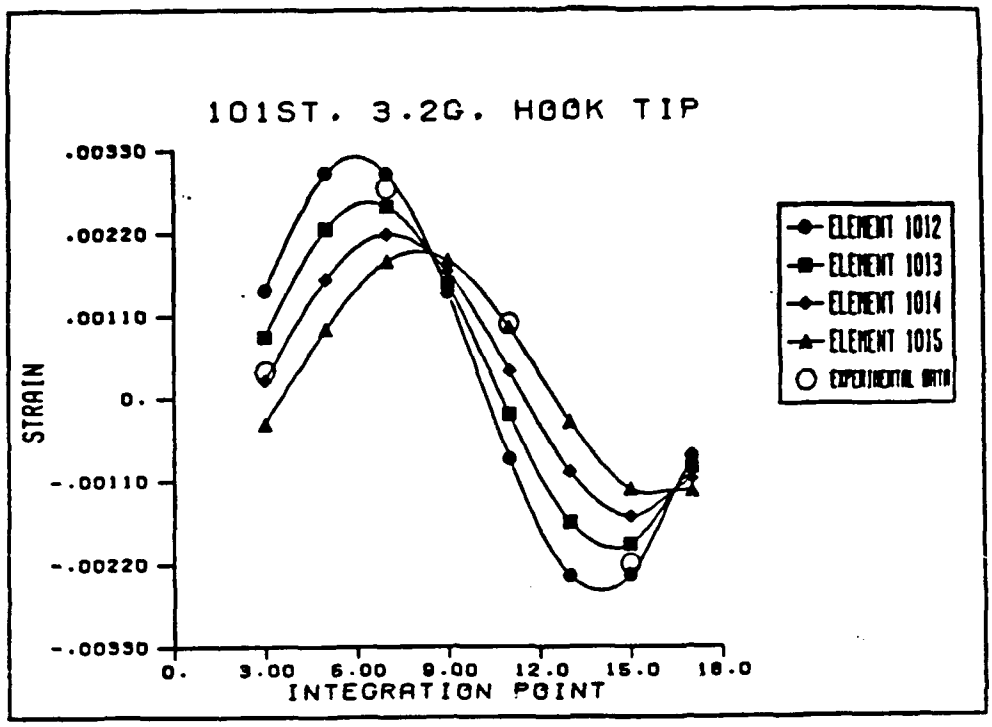

Figure 17. Elastic-plastic 3.2g FEA results for forward portion of hook in 101st configuration. Corresponding strain gage results superimposed all at 3.2g.

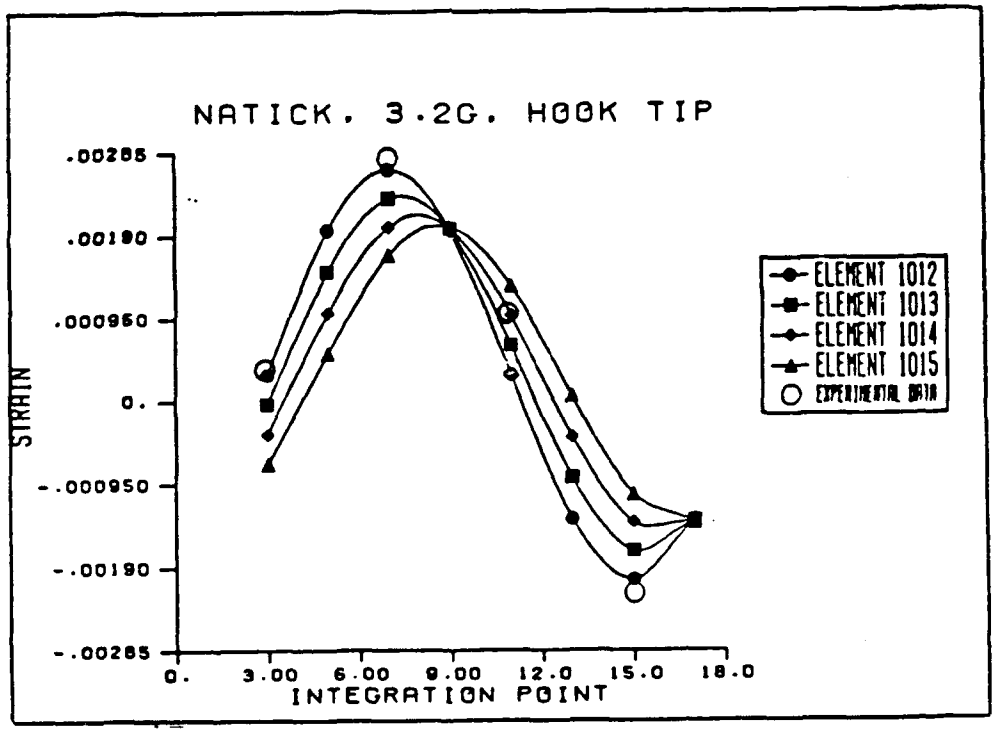

Figure 18. Elastic-plastic 3.2g FEA results for forward portion of hook in NRDEC configuration. Corresponding strain gage results superimposed all at 3.2g.

Figures 15 and 16 shows the four curves generated by the beam element integration points as a function of the element number along the curved portion of the hook. Figure 15, representing the 101st configuration shows a large number of element integration point strains whose absolute values exceed the 2.966E-03 in/in yield strain failure limit. The NRDEC case (Figure 16), to a lesser degree than the 101st, shows failure at the forward hook/bracket weld interface and chain/hook contact point.

Finite element analysis results of the forward straight section of the "U" shaped rod were compared to the front strain gage band, consisting of gages no. 12 - 15. Figures 17 and 18 show the correlation between experimental and FEA results for the 101st and NRDEC configurations respectively. For these plots, integration point identification numbers (3,7,11,15) are plotted along the abscissa versus strain. These beam element integration point locations were the intended locations of the forward strain gage band. Slight slippage occurred during gage bonding resulting in gage location changes both circumferentially and longitudinally.

Contour plots of the bracket section of the provision were generated for both configurations. No attempt was made to correlate these results with data obtained via strain gages number 1 through 5. Photographs taken of the bracket section lacked the necessary detail and clarity required to accurately estimate the coordinates of the gages in that section. Results do however predict that failure by yielding would occur at bracket locations close to the frame bolt holes at 3.2g loads in both configurations. Contour plot results for both configurations are shown in Figures 16.

MODEL SENSITIVITY OBSERVATIONS AND ANALYSIS

Strain gage data files, processed prior to the statistical sampling and averaging procedure, indicated a discrepancy between the two 101st configuration lift tests. Graphical methods of strain value determination for these two tests resulted in the values shown in Table 4.

Close examination of the data on a gage-by-gage basis revealed an apparent trend in magnitudes of strain between the two files. Repeatability of strain readings for most out-of-plane sensing strain gages was relatively high for the two 101st configuration lift tests. This trend indicates that the sensitivity of the hook to small changes in out-of-plane loads (F_z) is small. Repeatability of in-plane sensing strain gages on the other hand was poor. This trend would indicate that the sensitivity of the hook to small changes in the vectorial sum of in-plane ($\Sigma F_x + F_y$) forces is high

Table 4. STRAIN GAGE RESULTS FOR TWO TESTS OF THE 101st CONFIGURATION.

GAGE #	R03 $\mu\epsilon$	R04 $\mu\epsilon$	$\lvert\delta\rvert$ $\mu\epsilon$	location ip/op **
1.	-134	-135		na
2.	-105	-102		na
3.	20	20		na
4.	-95	-100		na
5.	-100	-100		na
6.	900	910	10	op
7.	515	398	117	ip
8.	-767	-770	3	op
9.	-150	-81	69	ip
10.	255	343	88	ip
11.	-64	-131	67	ip
12.	880	930	50	op
13.	112	65	47	ip
14.	-611	-670	59	op
15.	315	390	75	ip

** "ip" indicates gages sensing in-plane bending strains, "op" indicates gages sensing out-of-plane bending strains.

In light of these apparent trends, and the fact that the second 101st configuration lift test (R04) was not intended to yield high quality (stabilized vehicle motion) results, an FEA model sensitivity analysis was performed.

Table 5 lists, in a columnwise fashion, the integration point strain results for element number 44 of the linear elastic 101st configuration FEA model. This model was loaded with the appropriate 3.2g force, and executed five times (once for each of the five loaded node numbers identified). The total horizontal span between the extreme nodes, #16 and #20, is 0.7454 inches.

Percent variation calculations were then performed to determine the percent change in axial strain between the highest and lowest reported strain values for each of the four integration points. The results of these calculations are displayed in Table 6.

Table 5. FEA STRAIN RESULTS OF ELEMENT NUMBER 44 AS A FUNCTION OF LOADING NODE.

Loaded Node #	I.P. #3 ($\mu\epsilon$)	I.P. #7 ($\mu\epsilon$)	I.P. #11 ($\mu\epsilon$)	I.P. #15 ($\mu\epsilon$)
16	-1325	1645	1798	-1172
17	-1340	1823	1878	-1294
18	-1318	2052	1935	-1435
19	-1278	2201	1951	-1529
20	-1204	2377	1943	-1638

Table 6. PERCENT VARIATION OF FEA STRAIN RESULTS PER INTEGRATION POINT.

Integration Point	Force Application Nodes	Distance (in)	δ%
3	17/20	0.565	11.3
7	20/16	0.745	44.5
11	19/16	0.554	8.5
15	20/16	0.745	39.8

In the worst case, integration point #7 results vary by as much as 44.5 % when adjusting the loading position of the model by a corresponding 0.745 inches. Both integration points number 7 and 15 report bending induced axial strains for the out-of-plane direction. Referring to Table 4, the differences of 50 and 59 microstrain corresponding to out-of-plane gages #12 and #14 (element #44 vicinity) respectively, could be attributable to inconsistent chain/hook contact positions between the two tests. To a lesser degree, and as predicted by the model, in-plane strain discrepancies would also result from adjusting the contact position of the sling/chain to the hook during testing.

CONCLUSIONS

Simulated DSS airlift tests were performed to characterize the forward outboard sling force vector for both DSS configurations. Experimental 1.0g FO sling forces were found to be 2,913 lbs for the 101st configuration and 2,435 lbs for the NRDEC configuration. Sling force vector resolution calculations were performed using two methods. Results of the calculations were used to resolve the sling force into mutually orthogonal components relative to a coordinate axes system originating at the chain hook contact point. Results of component inspection indicated that the NRDEC configuration loads the provision more efficiently than the 101st configuration. The excessive rearward in-plane load (F_x = - 617 lbs) applied by the 101st configuration FO sling, induces bending stresses, which when extrapolated to 3.2g loads and superimposed with axial stresses, create unacceptable levels of stress as stipulated by MIL-STD-209G.

Results of both FEA models predicted material yielding below the required 3.2g elastic limit as stipulated in MIL-STD-209G. The 101st configuration was found to fail at 2.62g by means of interpolation. A significant improvement over the 101st configuration failure load was observed with the NRDEC configuration, which by interpolation indicated failure at 3.18g.

Due to discrepancies found between two 101st configuration strain gage data files, a model sensitivity study was performed where sling load application points were adjusted over the bounds of a 0.75" horizontal distance. An element close to the forward hook/bracket weld was observed as the loading node was moved through the 0.75" range. Results of the study were similar to the behavior of the two 101st configuration data files which demonstrated that both the models and the actual hook itself are complex structures and are both extremely sensitive to loading points.

It was the intention of this investigation to determine if the two DSS configurations proposed for possible safety release conformed to MIL-STD-209G. FEA models used to determine material yielding correlated with experimental strain results at various locations to varying degrees. In both configurations, FEA models indicated that material yielding would occur at sling force magnitudes lower than the 3.2g limit set in MIL-STD-209G. The results imply that both configurations do not meet the requirements of MIL-STD-209G.

ACKNOWLEDGEMENTS

The authors would like to express their appreciation to Ronald Aghababian and Jashiema Roach of AMTL for their assistance in processing statistics and test data.

Special thanks to Andrew Mawn, Nancy Harrington and John Doucette of NRDEC for their assistance in planning, coordinating and participating in the simulated airlift tests.

BIBLIOGRAPHY

1. MIL-STD-209G; *Military Standard Slinging Tiedown Provisions for Lifting and Tying Down Military Equipment*, p. A-14 para 5.1.1.1.

2. ABAQUS, Version 4.7, Hibbet, Karlson, and Sorenson, Inc., Providence, R.I.

3. PATRAN, Version 2.5, PDA Engineering, Costa Mesa, CA.

4. Beatty J. H. 1LT, Cavallaro P.V., Pasternak R.E., et al, *Strain Analysis of HMMWV Front Lift Provision*, MTL Letter Report.

5. Cavallaro C., Dooley R.B., Weight K.D., Cavallaro, P., *Testing and Analysis of Modified HMMWV Front Lift Provision*, MTL Technical Report #92-31.

APPENDIX I

Sling Force Resolution Calculations

Method 1. Graphical determination of resolved forces.

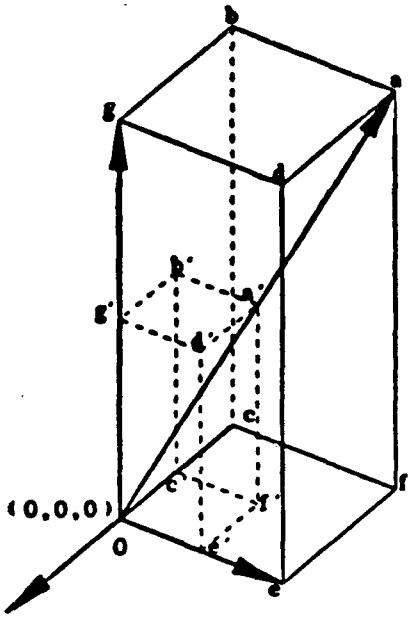

KNOWN:
1. Lift sling originates at (0,0,0) and terminates at point a.
2. Magnitude of sling force is 2,913 pounds.
3. Angle dOe is 72
4. Angle bOc is 8

SOLUTION:

1. Estimate Ob'as 100 units
2. Angle b'Og' is 8
3. Og'= 100 cos 8 = 99.03
   Oc'= 100 sin 8 = 13.92
4. Angle d'Oe' is 72
   Od' sin 72 = 99.03
   Od'= 104.13
   Oe'= 104.13 cos 72 = 32.18
5. $Oa' = SQRT (Oc'^2 + Oe'^2 + Og'^2) = 105.15$
   $Of' = SQRT (Oc'^2 + Oe'^2) = 35.06$

6. By similar triangles,

   Oa'/Of' = Oa/Of

   Of = (Oa x Of')/Oa' = (2913 x 35.06)/105.15
   Of = 971.28

7. Angle f'Oe' $\tan^{-1}$ (Oc'/Oe') = $\tan^{-1}$ (13.92/32.18)

   Angle f'Oe' = 23.39

   Angle c'Of' = 90 - 23.39 = 66.61

   *** Oe = Of cos 23.39 = 891.46 ***
   *** Oc = Of cos 66.61 = 385.59 ***

8. Oa'/Oa = Og'/Og

   Og = (Og' x Oa)/Oa' =(99.03 x 2913)/105.15

   *** Og = 2746 ***

9. Recall Of = 971.28

   angle fOc = $\tan^{-1}$ (Oe/Oc) = 66.61 degrees
   angle fOe = (90 - 66.61) = 23.39

10. Project coordinate of point f to axis rotated 16 degrees clockwise relative to axis Og.

    971.28 cos (66.61 - 16) = 617 (negative Oc direction)
    971.28 cos (23.39 + 16) = 751 (positive Oe direction)

11. The three resolved components of Oa are:

Og	= 2746
Oe (16 deg. rot.)	= 751
Oc (16 deg. rot.)	= 617

Axes Transformation Calculations

Input: Resolved forces in vehicle coordinate system.
Results: Resolved forces in hook coordinate system.
** Refer to pages 7,8,31.

Rotate about x-axis by (+θx):

$x' = x\underline{i} = x\underline{i}'$

$y' = y\cos\theta_x\underline{j} + y\sin\theta_x\underline{k}$

$z' = -z\sin\theta_x\underline{j} + z\cos\theta_x\underline{k}$

$$\begin{bmatrix} Fx' \\ Fy' \\ Fz' \end{bmatrix} = \begin{bmatrix} 1 & 0 & 0 \\ 0 & \cos\theta_x & \sin\theta_x \\ 0 & -\sin\theta_x & \cos\theta_x \end{bmatrix} \begin{bmatrix} Fx \\ Fy \\ Fz \end{bmatrix}$$

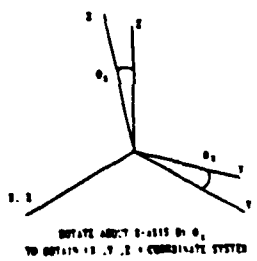

Rotate about y'-axis by (+$\theta_{y'}$):

$\underline{x}'' = x'\cos\theta_{y'}\underline{i}' - x'\sin\theta_{y'}\underline{k}'$

$\underline{y}'' = y'\underline{j}' = y'\underline{j}''$

$\underline{z}'' = z'\sin\theta_{y'}\underline{i}' + z'\cos\theta_{y'}\underline{k}'$

$$\begin{bmatrix} Fx'' \\ Fy'' \\ Fz'' \end{bmatrix} = \begin{bmatrix} \cos\theta_{y'} & 0 & -\sin\theta_{y'} \\ 0 & 1 & 0 \\ \sin\theta_{y'} & 0 & \cos\theta_{y'} \end{bmatrix} \begin{bmatrix} Fx' \\ Fy' \\ Fz' \end{bmatrix}$$

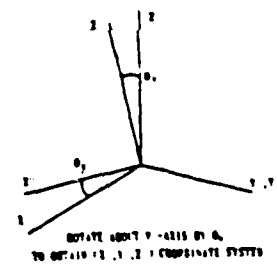

Rotate about z"-axis by (+$\theta_{z''}$):

$\underline{x}''' = x''\cos\theta_{z''}\underline{i}'' + x''\sin\theta_{z''}\underline{j}''$

$\underline{y}''' = -y''\sin\theta_{z''}\underline{i}'' + y''\cos\theta_{z''}\underline{j}''$

$\underline{z}''' = \underline{z}'' = z''\underline{k}'' = z''\underline{k}'''$

$$\begin{bmatrix} Fx''' \\ Fy''' \\ Fz''' \end{bmatrix} = \begin{bmatrix} \cos\theta_{z''} & \sin\theta_{z''} & 0 \\ -\sin\theta_{z''} & \cos\theta_{z''} & 0 \\ 0 & 0 & 1 \end{bmatrix} \begin{bmatrix} Fx'' \\ Fy'' \\ Fz'' \end{bmatrix}$$

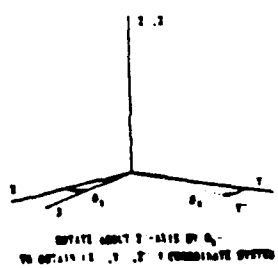

DISTRIBUTION LIST

No. of Copies	To
1	Office of the Under Secretary of Defense for Research and Engineering, The Pentagon, Washington, DC 20301
	Commander, U.S. Army Laboratory Command, 2800 Powder Mill Road, Adelphi, MD 20783-1145
1	ATTN: AMSLC-IM-TL
1	AMSLC-CT
	Commander, Defense Technical Information Center, Cameron Station, Building 5, 5010 Duke Street, Alexandria, VA 22304-6145
2	ATTN: DTIC-FDAC
1	MIA/CINDAS, Purdue University, 2595 Yeager Road, West Lafayette, IN 47905
	Commander, Army Research Office, P.O. Box 12211, Research Triangle Park, NC 27709-2211
1	ATTN: Information Processing Office
	Commander, U.S. Army Materiel Command, 5001 Eisenhower Avenue, Alexandria, VA 22333
1	ATTN: AMCSCI
	Commander, U.S. Army Materiel Systems Analysis Activity, Aberdeen Proving Ground, MD 21005
1	ATTN: AMXSY-MP, H. Cohen
	Commander, U.S. Army Missile Command, Redstone Scientific Information Center, Redstone Arsenal, AL 35898-5241
1	ATTN: AMSMI-RD-CS-R/Doc
1	AMSMI-RLM
	Commander, U.S. Army Armament, Munitions and Chemical Command, Dover, NJ 07801
2	ATTN: Technical Library
	Commander, U.S. Army Natick Research, Development and Engineering Center, Natick, MA 01760-5010
1	ATTN: Technical Library
	Commander, U.S. Army Satellite Communications Agency, Fort Monmouth, NJ 07703
1	ATTN: Technical Document Center
	Commander, U.S. Army Tank-Automotive Command, Warren, MI 48397-5000
1	ATTN: AMSTA-ZSK
1	AMSTA-TSL, Technical Library
	Commander, White Sands Missile Range, NM 88002
1	ATTN: STEWS-WS-VT
	President, Airborne, Electronics and Special Warfare Board, Fort Bragg, NC 28307
1	ATTN: Library
	Director, U.S. Army Ballistic Research Laboratory, Aberdeen Proving Ground, MD 21005
1	ATTN: SLCBR-TSB-S (STINFO)
	Commander, Dugway Proving Ground, UT 84022
1	ATTN: Technical Library, Technical Information Division
	Commander, Harry Diamond Laboratories, 2800 Powder Mill Road, Adelphi, MD 20783
1	ATTN: Technical Information Office
	Director, Benet Weapons Laboratory, LCWSL, USA AMCCOM, Watervliet, NY 12189
1	ATTN: AMSMC-LCB-TL
1	AMSMC-LCB-R
1	AMSMC-LCB-RM
1	AMSMC-LCB-RP
	Commander, U.S. Army Foreign Science and Technology Center, 220 7th Street, N.E., Charlottesville, VA 22901-5396
3	ATTN: AIFRTC, Applied Technologies Branch, Gerald Schlesinger
	Commander, U.S. Army Aeromedical Research Unit, P.O. Box 577, Fort Rucker, AL 36360
1	ATTN: Technical Library

No. of Copies	To
	Commander, U.S. Army Aviation Systems Command, Aviation Research and Technology Activity, Aviation Applied Technology Directorate, Fort Eustis, VA 23604-5577
1	ATTN: SAVDL-E-MOS
	U.S. Army Aviation Training Library, Fort Rucker, AL 36360
1	ATTN: Building 5906-5907
	Commander, U.S. Army Agency for Aviation Safety, Fort Rucker, AL 36362
1	ATTN: Technical Library
	Commander, USACDC Air Defense Agency, Fort Bliss, TX 79916
1	ATTN: Technical Library
	Commander, Clarke Engineer School Library, 3202 Nebraska Ave., N, Ft. Leonard Wood, MO 65473-5000
1	ATTN: Library
	Commander, U.S. Army Engineer Waterways Experiment Station, P.O. Box 631, Vicksburg, MS 39180
1	ATTN: Research Center Library
	Commandant, U.S. Army Quartermaster School, Fort Lee, VA 23801
1	ATTN: Quartermaster School Library
	Naval Research Laboratory, Washington, DC 20375
1	ATTN: Code 5830
2	Dr. G. R. Yoder - Code 6384
	Chief of Naval Research, Arlington, VA 22217
1	ATTN: Code 471
1	Edward J. Morrissey, WRDC/MLTE, Wright-Patterson Air Force Base, OH 45433-6523
	Commander, U.S. Air Force Wright Research & Development Center, Wright-Patterson Air Force Base, OH 45433-6523
1	ATTN: WRDC/MLLP, M. Forney, Jr.
1	WRDC/MLBC, Mr. Stanley Schulman
	NASA - Marshall Space Flight Center, MSFC, AL 35812
1	ATTN: Mr. Paul Schuerer/EH01
	U.S. Department of Commerce, National Institute of Standards and Technology, Gaitherburg, MD 20899
1	ATTN: Stephen M. Hsu, Chief, Ceramics Division, Institute for Materials Science and Engineering
1	Committee on Marine Structures, Marine Board, National Research Council, 2101 Constitution Avenue, N.W., Washington, DC 20418
1	Materials Sciences Corporation, Suite 250, 500 Office Center Drive, Fort Washington, PA 19034-3213
1	Charles Stark Draper Laboratory, 68 Albany Street, Cambridge, MA 02139
	Wyman-Gordon Company, Worcester, MA 01601
1	ATTN: Technical Library
	General Dynamics, Convair Aerospace Division P.O. Box 748, Forth Worth, TX 76101
1	ATTN: Mfg. Engineering Technical Library
	Plastics Technical Evaluation Center, PLASTEC, ARDEC Bldg. 355N, Picatinny Arsenal, NJ 07806-5000
1	ATTN: Harry Pebly
1	Department of the Army, Aerostructures Directorate, MS-266, U.S. Army Aviation R&T Activity - AVSCOM, Langley Research Center, Hampton, VA 23665-5225
1	NASA - Langley Research Center, Hampton, VA 23665-5225
1	U.S. Army Propulsion Directorate, NASA Lewis Research Center, 2100 Brookpark Road, Cleveland, OH 44135-3191
1	NASA - Lewis Research Center, 2100 Brookpark Road, Cleveland, OH 44135-3191
	Director, U.S. Army Materials Technology Laboratory, Watertown, MA 02172-0001
2	ATTN: SLCMT-TML
4	Authors

U.S. Army Materials Technology Laboratory
Watertown, Massachusetts 02172-0001
EVALUATION OF THE MODIFIED FORWARD HMMWV LIFT PROVISION IN DUAL SIDE-BY-SIDE AIRLIFT CONFIGURATIONS -
Robert B. Dooley, Paul V. Cavallaro, Kristen D. Weight, and Christopher Cavallaro

Technical Report MTL TR 92-65, September 1992, 35 pp, illus-tables, D/A Project 1L162105AH84

AD ____________

UNCLASSIFIED
UNLIMITED DISTRIBUTION

Key Words

High mobility multipurpose wheeled vehicles (HMMWV)
External airlift transport (EAT)
Airlift configuration

Field modifications to U.S. Army External Airlift Transport (EAT) operating procedures became critically necessary during Operation Desert Storm. To meet mission essential objectives, the U.S. Army 101st Airborne Division developed a new dual side-by-side (DSS) airlift sling configuration for airlifting two high mobility multipurpose wheeled vehicles (HMMWV) simultaneously with a CH-47D helicopter. The U.S. Army Materials Technology Laboratory performed experimental and finite element analysis (FEA) activities to evaluate the performance of the forward outboard HMMWV lift provisions subjected to DSS sling configurations. These activities were performed at the request of the Natick Research, Development, and Engineering Center in an attempt to certify two DSS airlift configurations under consideration for further use. Results of both the experimental and analytical analyses were obtained, discussed, and subsequently correlated. Conformity of the provision to Military Standard 209-G, "Slinging and Tiedown Provisions for Lifting and Tying Down Military Equipment" was evaluated for both configurations.

U.S. Army Materials Technology Laboratory
Watertown, Massachusetts 02172-0001
EVALUATION OF THE MODIFIED FORWARD HMMWV LIFT PROVISION IN DUAL SIDE-BY-SIDE AIRLIFT CONFIGURATIONS -
Robert B. Dooley, Paul V. Cavallaro, Kristen D. Weight, and Christopher Cavallaro

Technical Report MTL TR 92-65, September 1992, 35 pp, illus-tables, D/A Project 1L162105AH84

AD ____________

UNCLASSIFIED
UNLIMITED DISTRIBUTION

Key Words

High mobility multipurpose wheeled vehicles (HMMWV)
External airlift transport (EAT)
Airlift configuration

Field modifications to U.S. Army External Airlift Transport (EAT) operating procedures became critically necessary during Operation Desert Storm. To meet mission essential objectives, the U.S. Army 101st Airborne Division developed a new dual side-by-side (DSS) airlift sling configuration for airlifting two high mobility multipurpose wheeled vehicles (HMMWV) simultaneously with a CH-47D helicopter. The U.S. Army Materials Technology Laboratory performed experimental and finite element analysis (FEA) activities to evaluate the performance of the forward outboard HMMWV lift provisions subjected to DSS sling configurations. These activities were performed at the request of the Natick Research, Development, and Engineering Center in an attempt to certify two DSS airlift configurations under consideration for further use. Results of both the experimental and analytical analyses were obtained, discussed, and subsequently correlated. Conformity of the provision to Military Standard 209-G, "Slinging and Tiedown Provisions for Lifting and Tying Down Military Equipment" was evaluated for both configurations.

U.S. Army Materials Technology Laboratory
Watertown, Massachusetts 02172-0001
EVALUATION OF THE MODIFIED FORWARD HMMWV LIFT PROVISION IN DUAL SIDE-BY-SIDE AIRLIFT CONFIGURATIONS -
Robert B. Dooley, Paul V. Cavallaro, Kristen D. Weight, and Christopher Cavallaro

Technical Report MTL TR 92-65, September 1992, 35 pp, illus-tables, D/A Project 1L162105AH84

AD ____________

UNCLASSIFIED
UNLIMITED DISTRIBUTION

Key Words

High mobility multipurpose wheeled vehicles (HMMWV)
External airlift transport (EAT)
Airlift configuration

Field modifications to U.S. Army External Airlift Transport (EAT) operating procedures became critically necessary during Operation Desert Storm. To meet mission essential objectives, the U.S. Army 101st Airborne Division developed a new dual side-by-side (DSS) airlift sling configuration for airlifting two high mobility multipurpose wheeled vehicles (HMMWV) simultaneously with a CH-47D helicopter. The U.S. Army Materials Technology Laboratory performed experimental and finite element analysis (FEA) activities to evaluate the performance of the forward outboard HMMWV lift provisions subjected to DSS sling configurations. These activities were performed at the request of the Natick Research, Development, and Engineering Center in an attempt to certify two DSS airlift configurations under consideration for further use. Results of both the experimental and analytical analyses were obtained, discussed, and subsequently correlated. Conformity of the provision to Military Standard 209-G, "Slinging and Tiedown Provisions for Lifting and Tying Down Military Equipment" was evaluated for both configurations.

U.S. Army Materials Technology Laboratory
Watertown, Massachusetts 02172-0001
EVALUATION OF THE MODIFIED FORWARD HMMWV LIFT PROVISION IN DUAL SIDE-BY-SIDE AIRLIFT CONFIGURATIONS -
Robert B. Dooley, Paul V. Cavallaro, Kristen D. Weight, and Christopher Cavallaro

Technical Report MTL TR 92-65, September 1992, 35 pp, illus-tables, D/A Project 1L162105AH84

AD ____________

UNCLASSIFIED
UNLIMITED DISTRIBUTION

Key Words

High mobility multipurpose wheeled vehicles (HMMWV)
External airlift transport (EAT)
Airlift configuration

Field modifications to U.S. Army External Airlift Transport (EAT) operating procedures became critically necessary during Operation Desert Storm. To meet mission essential objectives, the U.S. Army 101st Airborne Division developed a new dual side-by-side (DSS) airlift sling configuration for airlifting two high mobility multipurpose wheeled vehicles (HMMWV) simultaneously with a CH-47D helicopter. The U.S. Army Materials Technology Laboratory performed experimental and finite element analysis (FEA) activities to evaluate the performance of the forward outboard HMMWV lift provisions subjected to DSS sling configurations. These activities were performed at the request of the Natick Research, Development, and Engineering Center in an attempt to certify two DSS airlift configurations under consideration for further use. Results of both the experimental and analytical analyses were obtained, discussed, and subsequently correlated. Conformity of the provision to Military Standard 209-G, "Slinging and Tiedown Provisions for Lifting and Tying Down Military Equipment" was evaluated for both configurations.